The Complex Ecosystem in Non Small Cell Lung Cancer Invasion

Seth Haney[1], Jessica Konen[2,3], Adam I. Marcus[3,4], Maxim Bazhenov[1]

[1]Department of Medicine, Division of Pulmonary, Critical Care & Sleep Medicine, University of California, San Diego, La Jolla, CA

[2]Department of Thoracic/Head and Neck Medical Oncology, The University of Texas MD Anderson Cancer Center, Houston, Texas, USA.

[3]Winship Cancer Institute, Emory University, Atlanta, GA

[4]Department of Hematology and Medical Oncology, Emory University, Atlanta, GA

Supported by: R01DC012943 (MB), R01CA142858 (AIM), R01CA194027 (AIM), R01CA201340 (AIM). SH is Postdoctoral Kirschstein-NRSA fellow supported by training award T32HL134632.

Abstract

Many tumors are characterized by genetic instability, producing an assortment of genetic variants of tumor cells called subclones. These tumors and their surrounding environments form complex multi-cellular ecosystems, where subclones compete for resources and cooperate to perform multiple tasks, including cancer invasion. Recent empirical studies revealed existence of such distinct phenotypes of cancer cells, leaders and followers, in lung cancer. These two cellular subclones exchange a complex array of extracellular signals where interplay between them demonstrates a symbiotic relationship at the cellular level. Here, we develop a computational model of the microenvironment of the lung cancer ecosystem to explore how the relationships between subclones can advance or inhibit cancer progression. We found that due to the complexity of the ecosystem, cancer growth may have very different dynamics characterized by the different levels of aggressiveness. By altering the signaling environment, we could alter the ecological relationship between the cell types and the overall dynamics of the cancer cells population. Specifically, inhibition of the feedbacks targeting leader type of the cancer cells had profound impact on the outcome of cancer growth. Our study predicts a complex division of labor between cancer cell subclones and suggests new treatment strategies targeting signaling within heterogeneous tumor cell populations.

Introduction

Lung cancer is the second most prevalent type of cancer causing over 150,000 deaths per year in the United States [1]. Insufficient progress has been made in achieving efficacious treatments. One of the main challenging barriers in developing new treatment strategies is the vast diversity of cancer. Heterogeneity exists between patients with the same tumor type, between tumor loci within a patient (i.e. metastases and primary tumor), and within the primary tumor itself [2,3]. Cancer is distinguished by loss of normal control over cell processes leading to genetic instability and unregulated growth. Genetic instability creates array of different clonal populations with different cell fitnesses, renewal and invasion potential [4]. Competition between different cancerous subclones and normal cell types sets the stage for classical ecological dynamics in the tumor microenvironment. The outcome of this process determines success of the tumor progression and its understanding may help discover novel treatment approaches [5,6].

Invasion of surrounding tissue, either locally or distally via metastasis, is a hallmark of cancer [7]. Extensive research has detailed that invasion is mediated by interactions between the tumor and extracellular matrix [8,9] and cancer-associated fibroblasts [10], but there is a lack of focus on the cooperative interactions between distinct cancer subclones. Indeed, in mouse models of lung cancer, collective invasion of cancer cells was shown to correspond markedly more successful metastasis [3,11–13], confirming the critical role of collective invasion in driving cancer progression.

We recently developed a novel image-guided genomics approach that allowed us to identify at least two distinct phenotypic cell types in lung cancer invasion packs: highly migratory *leader cells* and highly proliferative *follower cells* [14]. Genomic and molecular interrogation of purified leader and follower cultures revealed differential gene expression prompting distinguishing phenotypes. Specifically, leader cells utilized focal adhesion kinase signaling to stimulate fibronectin remodeling and invasion. Leader cells also overexpressed many components of the vascular endothelial growth factor (VEGF) pathway facilitating recruitment of follower cells but not the leader cell motility itself [14]. However, leader cells proliferated approximately 70% slower than follower cells due to a variety of mitotic deficiencies. These mitotic and doubling rate deficiencies could be corrected by addition of cell media extracted from follower only cell cultures. This led to conclusion that follower cells produce an unknown extracellular factor responsible for correcting mitotic deficiencies in leader cells. In sum, leader cells provide an escape

mechanism for followers, follower cells (and follower cell media only) help leaders with increased growth. Together, these data support a service-resource mutualism during collective invasion, where at least two phenotypically distinct cell types cooperate to promote their escape.

In this new study, we developed population-level computational model to explore impact of complex interactions between leaders and followers cell types on the cancer progression. The model implemented effects of critical signaling factors controlling communication between cell types and interaction between cancer cells and environment. We derive analytic boundaries dividing parameter space by critical changes to the dynamics of cancer growth. The analysis revealed that specific coordination between leaders and followers, through the signaling feedbacks, have a major impact on the dynamics. Our study predicts the critical role of specific signaling pathways involved in the symbiotic interaction between cancer subclones for the overall success of cancer progression.

Methods

Our model tracks the cell counts of leader cells, *L*, and follower cells, *F*, the concentrations of extracellular factors VEGF, *V*, an unidentified Proliferation factor, *P*, and Fibronectin, *N*, as well as the size of the domains for leader cells, Ω_L, and for follower cells Ω_F. Based on the available data [14], the following processes have been implemented. Leader cells can expand their domain, Ω_L, by secreting Fibronectin, which in turn relaxes competitive pressure on leader cell growth. Leaders also secrete VEGF, which is taken up by follower cells and causes follower cells to follow them. This was modeled by increasing the domain for follower cells, which in turn relaxes competitive pressure on follower cells. Follower cells secrete an unknown proliferation signal that increases the reproductive capacity of leader cells (initially smaller than follower cells). Leader and follower cells also must compete with each other for resources at rate *c* (see Figure 1).

We modeled cell counts (*L* and *F* species) as standard Lotka-Volterra competition [15]. The carrying capacity of the leader cells was dynamic and dependent on the amount of proliferative signal, *P*, present. This capacity increased in a saturating manner with *P*, with maximum equal to the follower cell carrying capacity, K_{F0}. Intra- and inter-specific competition was driven by concentration, i.e. $[L]=L/\Omega_L$, and birthrate was driven by absolute number, *L*. The extracellular species (*V*,*P*,*N*) and domain sizes all had linear dynamics for simplicity. Below primes denote the time derivative of the variable.

$$\frac{L'}{L} = r_L\left[1 - \frac{(L/\Omega_L)+c(F/\Omega_F)}{K_{L0}+(K_F-K_{L0})\left(\frac{P}{\delta+P}\right)}\right] \quad (1)$$

$$\frac{F'}{F} = r_F\left[1 - \frac{(F/\Omega_F)+c(L/\Omega_L)}{K_F}\right] \quad (2)$$

$$V' = \beta_V L - \gamma_V V \quad (3)$$

$$P' = \beta_P F - \gamma_P P \quad (4)$$

$$N' = \beta_N L - \gamma_N N \quad (5)$$

$$\Omega_L{}' = \beta_{OL} N - \gamma_{OL}(\Omega_L - \Omega_{L0}) \quad (6)$$

$$\Omega_F{}' = \beta_{OF} V - \gamma_{OF}(\Omega_F - \Omega_{F0}) \quad (7)$$

Here r_L and r_F denote the rate of expansion for leaders and followers, respectively. The parameter c denotes the strength of competition between the two cell types. The capacity of the environment for follower cells is given by the parameter K_F. The capacity for leaders depended on an initial capacity, K_{L0}, and on the amount of proliferation signal in a Hill-like manner with EC50, δ. Each extra-cellular species (*V,P,N)* had a production rate, β, and a degradation rate γ, the domain size variables (Ω_L and Ω_F) also had a parameter denoting initial capacity (Ω_{L0} and Ω_{F0}).

Reduction and Feedbacks.

Previous 3D spheroid experiments show that invasion occurs on a much faster time scale than reproduction [14]. By assuming that factors (*V*,*P*,*N*) and domains (Ω_L, Ω_F) change much faster than cell counts, one can reduce these equations to a set of two equations (*L*,*F*), where variables in equations (3)-(7) are at their equilibria

$$V_{SS} = \frac{\beta_V}{\gamma_V} L; \qquad P_{SS} = \frac{\beta_P}{\gamma_P} F; \qquad N_{SS} = \frac{\beta_N}{\gamma_N} L; \qquad \Omega_L^{SS} = \frac{\beta_{OL}}{\gamma_{OL}} N; \quad \Omega_F^{SS} = \frac{\beta_{OF}}{\gamma_{OF}} V; \tag{8}$$

Using this reduction drastically reduced the complexity of the system. We also characterized the feedbacks based on the reduced system. The feedback that determines the leaders impact on their own domain expansion we denote by $s_L = \frac{\beta_N \beta_{OL}}{\gamma_N \gamma_{OL}}$, for the strength of the leader only feedback. The feedback that determines the leaders impact on follower cell growth we denote by $s_{LF} = \frac{\beta_V \beta_{OF}}{\gamma_V \gamma_{OF}}$, for the strength of the leader to follower feedback. The feedback that determines the followers impact on leader cell growth we denote by $s_{FL} = \frac{\beta_P}{\gamma_P \delta}$, for the strength of the follower to leader feedback.

Using these assumptions we can re-write the leader follower system as

$$\frac{L'}{L} = r_L \left[1 - \frac{\left(L/\Omega_L^{SS}(L)\right) + c\left(F/\Omega_F^{SS}(L)\right)}{K_L(F)}\right] \tag{9}$$

$$\frac{F'}{F} = r_L \left[1 - \frac{\left(F/\Omega_F^{SS}(L)\right) + c\left(L/\Omega_L^{SS}(L)\right)}{K_F}\right] \tag{10}$$

where

$$\Omega_L^{SS}(L) = s_L L + \Omega_{L0}; \quad \Omega_F^{SS}(L) = s_{LF} L + \Omega_{F0}; \quad K_L(F) = K_{L0} + (K_F - K_{L0}) \frac{s_{LF} F}{1 + s_{LF} F}.$$

Using this reduction we can derive several critical points in cancer growth. The reduced system (9),(10) has five equilibrium points: extinction of leaders, followers, both, and two coexistence points (where both leaders and followers populations are positive). Changes in feedback strengths cause fundamental shifts in cancer dynamics. We used parameter values $\Omega_L = 1, \Omega_F = 1$. To match experimental observations that leader cells grow slower and less effeciently, we set $r_L = 0.3$ and $K_{L0} = 0.3$ while $r_F = 1$ and $K_F = 1$. The strengths of the various feedbacks, s_L, s_{LF}, and s_{FL} are varied systematically below.

Transcritical Bifurcation at Zero

To determine the critical points in the leader follower system, we calculated the Jacobian of the reduced system when it is evaluated at Leader extinction ($L = 0, F = F_{LE} = \Omega_F \cdot K_F$).

$$J|_{L=0;F=F_{LE}} = \begin{pmatrix} r_L\left(1 - \frac{cK_F}{K_L^{SS}}\right) & 0 \\ r_F\left(\frac{K_{F0}s_F}{\Omega_{F0}^2} - \frac{c}{\Omega_{L0}}\right) & -r_F \end{pmatrix} \quad (11)$$

Here $K_L^{SS} = K_{L0} + \Omega_{F0}K_F\frac{\Omega_{F0}K_F}{\delta + \Omega_{F0}K_F}$, the value of K_L when $F = F_{LE}$. The Jacobian has eigenvalues

$$\lambda = \left[r_L\left(1 - c\frac{K_{F0}}{K_L^{SS}}\right), -r_F\right] \quad (12)$$

Thus, extinction of Leaders is stable as long as $c > \frac{K_L^{SS}}{K_{F0}}$, which determines an upper bound on competition where Leader and Followers can coexist and a bifurcation in our system we call the transcritical bifurcation at zero.

Saddle Node Bifurcation

The system also undergoes a saddle node bifurcation when s_L increases beyond the point where any coexistence equilibrium points exist. In this case, the leader/follower system undergoes unbounded growth. This bifurcation was determined numerically using MatCont [16]. We found that this point depended critically on both the leader feedback

strength, s_L, and on the competition strength, c. One of these coexistence points is effected by the transcritical bifurcation, below.

Transcritical Bifurcation at Infinity

When the leader feedback strength is sufficiently high relative to competition, leaders and followers will undergo unbounded growth from certain regions of phase space. We describe this scenario as an attractor basin in phase space for the infinity attractor. However, if s_L is reduced (or c is increased) beyond a certain threshold, infinity becomes unstable. This corresponds precisely with the loss of an unstable equilibrium point with non-zero values of both leaders and followers. Leaders and followers that are coexisting must satisfy

$$\frac{L}{\Omega_L} + c\frac{F}{\Omega_F} = K_L(F) \tag{13}$$

and $\frac{F}{\Omega_F} + c\frac{L}{\Omega_L} = K_F$ or equivalently,

$$\frac{F}{\Omega_F} = K_F - c\frac{L}{\Omega_L}. \tag{14}$$

In the case that follower populations are large relative to δ, $K_L(F) \to K_F$, we substituted (13) into (14) to find

$$L = \frac{K_F \Omega_{L0}}{(1+c)\left(1-\frac{K_F s_L}{1+c}\right)} \tag{15}$$

which has a discontinuity at

$$c > K_F s_L - 1 \tag{16}$$

defining the loss of one of the coexistence equilibrium points where both L and F are large. We describe this as the transcritical bifurcation at infinity as the stability of infinity changes around this point.

Results

Leader and Follower System

Leader and follower cancer cell types in non-small cell lung cancer spheroids were previously isolated using a fluorescence technique [14] (Figure 1A,B). We found that leaders and followers are genotypically and phenotypically distinct populations of cancer cells that exchange a variety of signaling molecules to coordinate complex behavior during invasion. In this new work we focus on four main channels of communication. Leader cells secrete fibronectin in an autocrine manner. This leads to ECM restructuring and expansion of leader cell domain, Ω_L, (see Methods) which ultimately increases the leader cell count. The strength of this positive feedback is characterized in our model by s_L (strength of Leader-only feedback). Leader cells also secrete VEGF. In the leader follower ecosystem this promotes follower cells to track expanding leader cells, increases follower domain size (Ω_F), and ultimately, follower cell count. In our model, the strength of this feedback is given by s_{LF} (strength of Leader to Follower feedback). Follower cells secrete an undetermined proliferation signal, as evidenced by the observation that follower-only cell media increases leader cell growth rate [14]. The strength of this feedback is given by s_{FL} (strength of Follower to Leader feedback) in our model. Finally, both cell types compete for resources modeled here by the feedback c (see Figure 1C).

These feedbacks were incorporated into a modified Lotka-Volterra competition-cooperation model. We chose a Lotka-Volterra model to focus on the ecological aspects of competition in the cancer ecosystem. Here, the leader cells could grow to a total capacity K_L, which is an increasing function of the proliferation signal secreted by follower cells. This capacity was reached when a combination of leader and follower cell densities (counts divided by domain) exceeds K_L (see Methods). Increases in the domains of each type (by Fibronectin secretion in the leader case and VEGF in the follower case) limited the overall density of that cell type and mitigated its impact on the overall capacity of the system. Increasing competition, for example by limiting resources, increased the impact of either cell type on the conjugate capacity type (e.g. how leader density, L/Ω_L, impacts follower capacity K_F).

This system of feedbacks between leader and follower cells describes a complex ecosystem. The impact these feedbacks may have on cacner growth or invasion is unclear. Leader and follower cells engage in competition for resources but also be engage in

supportive roles. Invasive leader cells provide new territory for leader cells and are supported by proliferative follower cells. We analyzed our model to find critical turning points for the ecosystem and cancer dynamics.

Multiple Types of Cancer Dynamics

We found that multiple feedbacks between leader and follower cell populations could produce a wide variety of dynamics. When competition strength was high and the strength of the leader only feedback, s_L, was moderate, limited growth resulted in a stable tumor bulk and size (Fig. 2A). However, when s_L was large and competition was moderate, dynamics displayed unbounded cancer growth (Fig. 2B). Intermediate values of both competition and s_L led to growth that depended on the initial tumor size: large tumors underwent unbounded growth, while small tumors attained a stable size (Figure 2C).

This complicated array of behavior can be explained by critical shifts in the cancer cell population dynamics due to the changes in the feedbacks strength. We found that depending on the level of competition, c, and the strength of invasiveness of leaders, s_L, the leader-follower ecosystem can operate in one of five different regimes, as described below (Figure 3).

Leader Extinction: When competition was high and invasive feedback was minimal, the leaders (the weaker competitor) were forced to extinction while follower cells persist. We found that this critical level of competition was given by $c > \frac{K_L^{SS}}{K_F}$ (see Methods, *Transcritical bifurcation at zero* for derivation). This critical level of competition, the ratio of the capacity of leader cells to that of the follower cells, is essentially is given by the fitness differences between leader only and follower only cell populations (Figure 3A,B). Thus, leader and follower populations with similar fitness would require a much higher competition threshold to drive the weaker competitor to extinction.

Leader Extinction with Escape: If competition was above the leader extinction limit $c > \frac{K_L^{SS}}{K_{F0}}$, but not high enough to balance the impacts of the leader only feedback, $c < K_F s_L - 1$, there were two possible outcomes depending on initial conditions (see Methods, *Transcritical Bifurcation at Infinity* for derivation). Leaders could go extinct if the population of leader cells was sufficiently small or if initial populations of leaders and followers were

large enough the tumor could grow unboundedly. These two outcomes are separated by a critical boundary (separatrix) where tumor bulk size determines its ultimate fate (Figure 3A,C). In this scenario, our model predicts, that the ability to undergo collective invasion depends on whether the initial tumor size is bigger than a critical amount. These dynamics with divergent outcomes occurs when competition is large enough to drive leaders extinct, but small enough to be outbalanced by the strong invasive effects of leader cells.

Benign Disease: When competition was smaller than the extinction limit, $c < \frac{K_L^{SS}}{K_{F0}}$, but large enough to balance leader feedback strength, $c > K_F s_L - 1$, leaders and followers attained a stable tumor size (Figure 3A,D). We refer to this as benign disease as the cancer cannot grow beyond a defined size. In this case, while competition was present, it was too weak to lead to extinction, while leader population was not invasive enough to promote unlimited growth. This scenario represents stable, non-invasive cancer.

Multimodal Disease: If competition was (a) small enough to allow leader existence, $c < \frac{K_L^{SS}}{K_{F0}}$, (b) small enough relative to leader feedback strength, so that escape was possible, $c < K_F s_L - 1$, but (c) high enough, so that for small initial population of leader it could balance the positive leader feedback (Figure 3A,E), leader and follower cell dynamics depended on initial tumor bulk size. For example, a large tumor will grow without bound but a small tumor will contract to a stable fixed size, due to competition as in benign disease. This critical boundary was defined by a separatrix of a saddle fixed point (Fig. 3E). This separatrix was determined numerically by reversing time [17].

Aggressive Disease: When leader invasive strength was sufficiently high and competition was sufficiently low, the only possible outcome was unbounded growth (Figure 3A, F).

This analysis revealed that complex feedbacks in the leader-follower cancer ecosystem may lead to the multiple types of cancer dynamics. When the leaders' invasiveness was low, the outcome depended on the competition between two populations – strong enough competition promoted leader extinction, while low competition allowed stable tumor size with both leader and follower cells. As leader invasiveness rate increased, the system revealed a new state with unlimited growth. This aggressive disease state coexisted with possibility of a limited size tumor when

competition between leaders and followers was strong enough. Otherwise, unlimited tumor growing was the only outcome.

How does the ecosystem respond to perturbations in these feedbacks? What are critical perturbations that would have profound changes in the ecosystem? We will discuss these questions next.

Blocking s_L Led to Irreversible Changes in Invasion

In multimodal disease, cancers can undergo explosive growth or achieve a stable tumor bulk size depending on the initial size of the tumor. We examined the impact of limiting the invasive leader feedback in cancers of this type. Even when the tumor was sufficiently large to support unbounded growth, after blocking invasive leader feedback s_L, the ecosystem was forced into the benign disease type and thus converged onto a stable tumor size (Figure 4 A-E). This stable tumor size persisted after restoring s_L to its original strength (Fig. 4E). From the point of view of bifurcation analysis, reducing leader feedback changed the systems structure so only a fixed attractor existed (Fig. 4A). In this regime, unlimited growth (Fig. 4B) was terminated and the system reached the attractor (Fig. 4C), which remained stable even after the feedback was restored to its original level (Fig. 4D).

These model predictions are consistent with in vitro data. Using siRNA blocking we previously showed that under expression of fibronectin (characterized by the strength of Leader-only feedback, s_L, in the model) led to limited invasion potential and stable tumor size (Fig. 4F) [14].

Increasing Competitive Signals Leads to Leader Extinction

Another impactful perturbation to affect the dynamics of the leader-follower ecosystem was to increase competition. Leader cells excrete extracellular factors that induce the death of followers and leaders alike. In our model, increasing competition led to irreversible leader extinction. Starting from aggressive disease type, we then increased competition parameters that caused the ecosystem change into extinction with escape type (Fig. 5A). This caused leader extinction to become stable and, given a complete eradication of leader cells (i.e. $L = 0$), persisted even after the removal of treatment (Fig.

5E). Again, this dynamic can be understood from perspective of the bifurcation analysis. After competition was increased (Fig. 5A), initial growth (Fig. 5B) was reversed as long as tumor was yet sufficiently small so the system remained in the attractor vicinity of the stable equilibrium representing stable tumor size (Fig. 5C).

Support For Leaders has Large Impact on Aggressiveness

Changes in the feedback strengths that determine the interaction between leaders and followers (s_{LF} and s_{FL}) also impact cancer dynamics. Leader cells secrete VEGF that help followers expand their territory (denoted here by s_{LF}) and follower cells secrete a proliferation signal that allows leaders to increase their proliferative capacity (denoted here by s_{FL}). These two feedbacks have distinct impacts on the overall dynamics of the cancer. Perturbations to s_{LF} (changing the impact that leaders have on followers) change dynamics by changing the location of the saddle node bifurcation boundary that separated state with unlimited growth only dynamics and a state with coexistence of the unlimited growth and stable tumor size regimes. Decreasing s_{LF} increased the threshold on invasion (s_L) needed to cause unbounded growth (Fig. 6A). We have exploited this to show that decreasing s_{LF} can cause decreases tumor bulk but these effects are reversed upon return to original s_{LF} levels (Fig. 6E). Indeed, reducing s_{LF} reversed unlimited tumor growth and put the system to the state with stable tumor size attractor (assuming that the tumor was small enough at the time of intervention) (Fig. 6 B,C). This regime persisted as long as feedback from the leaders to followers remained low. However, increasing s_{LF} restored the system dynamics with infinity being the only stable attractor and reversed growth (Fig. 6E)

We found that perturbations to s_{FL}, which affect the effect that followers have on leaders, have a much more significant impact on cancer dynamics. In contrast to s_{LF}, changes to the s_{FL} changed both the location of the saddle node bifurcation boundary and the transcritical bifurcation boundary of leader extinction (Fig. 7A). Therefore, decreasing s_{FL} both increased the threshold on the leader invasion strength (s_L) needed to cause unbounded growth and decreased the threshold of competition needed to induce leader cell extinction in the cancer system. We have exploited this to show that decreasing s_{FL} can cause irreversible decreases in tumor bulk due to stabilizing leader extinction (Fig. 7F). Again, starting with unlimited growth (Fig. 7B), decreasing followers to leaders' feedback s_{LF}, triggered the system convergence to the stable attractor – stable tumor size

(Fig. 7C). When the feedback was restored, the tumor size remained small enough to avoid regime of unlimited growth (Fig. 7D). In more general case, the outcome depended on the balance between the leader to follower, s_{FL}, and follower to leader, s_{LF}, feedbacks, with higher s_{LF} requiring more significant s_{FL} decrease to avoid unbounded growth (Fig. 7E).

Summary of Perturbations to Cancer Ecosystem

The complex feedback structure of the cancer ecosystem allows for the possibility of many different manipulations to have critical impacts on cancer dynamics. We reviewed each of the different possibilities in Table 1 from the perspective of trying to reduce tumor bulk. Hence, manipulating s_L, s_{LF}, s_{FL} should be interpreted as decreasing these feedbacks, whereas manipulating c should be interpreted as increasing c. We also examined the possibility of non-targeted cell death, such as might occur during non-specific chemotherapy. Manipulations were either irreversible upon cessation of the perturbation (e.g. Irreversible leader extinction and Irreversible stabilization of tumor) or simply cause reversible reduction in tumor bulk. In both the leader exctinction with escape and multimodal disease (see Figure 3) the size of the tumor dictates possible outcomes from the state. A state of “unbounded growth” denotes that the tumor bulk exceeds the critical amount and will grow unboundedly, “stable growth” denotes tumors are less than this value.

Type of dynamics	State	Manipulation Type	Outcome
1. Leader Extinction	N/A	death, c, s_L, s_{LF}, s_{FL}	Reversible tumor bulk reduction..
2. Leader Extinction w/ Escape	Unbounded growth	death s_L	Irreversible leader extinction.
		c, s_{LF}, s_{FL}	Reversible tumor bulk reduction.
	Stable growth	death c, s_L, s_{LF}, s_{FL}	Reversible tumor bulk reduction.
3. Benign Disease	N/A	c, s_{FL}	Irreversible leader extinction.
		s_L, s_{LF}, death	Reversible tumor bulk reduction.
4. Multimodal Disease	Unbounded growth	c, s_{FL}	Irreversible leader extinction.
		s_L, s_{LF}, death	Irreversible stabilization of tumor.
	Stable growth	c, s_{FL}	Irreversible leader extinction.
		s_L, s_{LF}, death	Reversible tumor bulk reduction.
5. Aggressive Disease	N/A	c, s_{FL}	Irreversible leader extinction.
		s_L, s_{LF}, death	Reversible tumor bulk reduction.

Table 1: Manipulation of different feedbacks impacts treatment. Manipulations were either irreversible upon cessation of the perturbation (e.g. Irreversible leader extinction and Irreversible stabilization of tumor) or simply cause reversible reduction in tumor bulk. In both the leader extinction with escape and multimodal disease (see Figure 3) the size of the tumor dictates possible outcomes from the state. A state of “unbounded growth” denotes that the tumor bulk exceeds the critical amount and will grow unboundedly, “stable growth” denotes tumors are less than this value.

Discussion

Heterogeneity of tumors, at the genetic, epigenetic, and phenotypic levels, is one of the main obstacles to developing new effective treatment strategies. Tumor cells rapidly evolve forming highly efficient symbiotic systems with well-defined labor division targeted to augment tumor survival and expansion. In lung cancer collective invasion packs, two distinct populations of cancer cells - highly migratory *leader cells* and highly proliferative *follower cells* – have been recently identified [14]. In this new study, we used computational models to explore collective dynamics of the leader-follower ecosystem and to explore approaches that can effectively disrupt it.

We found that competition between two populations (defined by the limited amount of resources), the positive feedback within the leader cell population (controlled by the focal adhesion kinase and fibronectin signaling) and impact of the follower cells to the leaders (represented by yet undetermined proliferation signal) all had major effects on the outcome of the collective dynamics. While increase of the positive feedback within the leader cell population would ultimately lead to the system state with unbounded tumor growth, manipulating follower to leader feedback or increasing competition between leader and follower cell populations was able to reverse this dynamic and to form a stable tumor configuration.

Our model highlights the importance of focal adhesion kinase (FAK) and fibronectin signaling. Our previous work showed that FAK signaling was a key distinguishing feature between leader and follower cells and critical for invasive leader behavior [14]. In our model FAK is the main driver of invasion by leader cells and disruptions in the FAK driven feedback loop, via strength s_L, cause critical changes in leader follower tumor dynamics. Indeed, FAK is a well-known regulator of the tumor micro-environment: promoting cell motility and invasion [18]. FAK expression is upregulated in ovarian [19] and breast cancer [20] tumors with expression levels correlating with survival [21,22]. Many FAK inhibitors, such as defactinib, are currently in clinical trials with promising results [18,23,23–27]. A key advantage of FAK inhibitors is that these will impact both in the tumor itself and the surrounding stroma where tumor associated fibroblasts also utilize FAK signaling to promote tumor invasiveness [28,29].

While commonly associated with angiogenesis in healthy and cancerous tissue, our previous work showed that VEGF mediates communication between leader and follower cells [14]. There is a long history of targeting VEGF to limit tumor invasiveness [30,31]. While great success has been seen in preclinical models [32,33], only moderate success was seen in clinical trials with anti-VEGF drugs such as bevacizumab [34,35]. This is largely due to cancers developing resistance to specific VEGF-therapeutics. In our model, VEGF stimulated followers to shadow leaders and expand their domain. However, we found that inhibition of VEGF had little impact on tumor dynamics relative to perturbations on other axes (such as FAK or competition).

Competition for resources is one of the fundamental forces that structures any ecosystem, including tumor ecosystems [6,36]. Our modeling work suggested that competition was a critical component in the leader follower ecosystem. We showed that when the strength of competition exceeded a critical threshold, leaders (the weaker competitor) were driven to extinction. Further, enhancements in competition changed the fundamental dynamics of the tumor. In some cases this meant stopping unbounded growth and promoting the extinction of leader cells. In addition to abstract competition, our previous work demonstrated that leaders actually inhibit the growth of followers through an unknown secreted factor in cell media [14]. While still in the early stages, exploiting this inhibition may also provide similar benefits to those shown here as increases in competition.

Our previous also revealed a currently unknown extracellular factor secreted by followers that corrects mitotic deficiencies and enhances leader proliferation [14]. Our modeling highlights this factor as having critical impact on tumor dynamics. We found that blockade of this proliferation factor, modeled here by s_{FL}, can cause multiple different critical shifts in tumor dynamics. More work needs to be done to identify and understand the mechanism of this factor, but preliminary results reveal that this may be a novel treatment axis that specifically targets the mutualistic action between leaders and followers.

Ecological forces shape the exchange of biomaterial between different biotic and abiotic environmental agents. These forces determine capacity of the ecosystem for different species (subclones) and the environment ultimately sets the fitness of each of the competitors. Classic ecological theory dictates that an abundance of many similar

species (such as similar subclonal populations) will lead to a high competition for resources [37,38]. This competition can force the exclusion of inferior competitors and ultimately may reduce heterogeneity of the system. However, when symbiotic and mutualistic interactions occur, otherwise competitive species support each other and increase the capacity of the ecosystem [39,40]. Symbiosis between different subclonal populations may be particularly important during critical times when the tumor survival is in peril (such as hypoxia, metastasis or therapy). One critical moment in tumor progression occurs when highly proliferative tumor cells saturate the resource potential of their current environment. In order to obtain more resources, tumors need to invade new territory.

Previous results to model complex tumor cell population dynamics range from very detailed cellular level models (e.g. [9,41–43]) to continuous models with a different degree of complexity (e.g. [44–48]) similar to that proposed in our new study. While cellular level model can directly incorporate heterogeneous cell types and intrinsic tumor properties, including proliferation, metabolism, migration, protease and basement membrane protein expression, and cell-cell adhesion, they have a high-dimensional state variables and parameter space that is difficult to analyze. Advantages of the reduced type of models include the low dimensional parameter space, where parameters have clear biophysical meanings, and which allows for systematic analysis to rapidly explore and determine the sensitive parameter space. We previously applied this approach to study cell interactions in chronic cancers and predicted conditions for explosive tumor growth [44]. Similar approach was applied to study cancer cell population dynamics in other types of cancers [45,48,49].

Conclusions:

The vast diversity both between different cancers and within a single tumor remains one of the biggest hurdles to overcome to achieve personalized cancer treatment. This diversity leads to a complex array of interactions between different tumor cell types and the healthy surrounding tissue: the tumor ecosystem. Our work has isolated phenotypically unique lung cancer cells and taken a dynamical approach to understanding the interactions within the tumor ecosystem. In this new study, we identified the critical

461 features and interactions composing the leader-follower ecosystem, to explore
462 vulnerabilities of the lung cancer invasive cell populations.

463

1. American Cancer Society. Cancer Facts & Figures 2016.

2. Burrell RA, McGranahan N, Bartek J, Swanton C. The causes and consequences of genetic heterogeneity in cancer evolution. Nature. 2013;501: 338–345. doi:10.1038/nature12625

3. Gerlinger M, Swanton C. How Darwinian models inform therapeutic failure initiated by clonal heterogeneity in cancer medicine. Br J Cancer. 2010;103: 1139–1143. doi:10.1038/sj.bjc.6605912

4. Greaves M, Maley CC. Clonal evolution in cancer. Nature. 2012;481: 306–313. doi:10.1038/nature10762

5. Korolev KS, Xavier JB, Gore J. Turning ecology and evolution against cancer. Nat Rev Cancer. 2014;14: 371–380. doi:10.1038/nrc3712

6. Pienta KJ, McGregor N, Axelrod R, Axelrod DE. Ecological Therapy for Cancer: Defining Tumors Using an Ecosystem Paradigm Suggests New Opportunities for Novel Cancer Treatments. Transl Oncol. 2008;1: 158–164.

7. Hanahan D, Weinberg RA. Hallmarks of Cancer: The Next Generation. Cell. 2011;144: 646–674. doi:10.1016/j.cell.2011.02.013

8. Ruoslahti E. The Walter Herbert Lecture. Control of cell motility and tumour invasion by extracellular matrix interactions. Br J Cancer. 1992;66: 239–242.

9. Bauer AL, Jackson TL, Jiang Y. Topography of Extracellular Matrix Mediates Vascular Morphogenesis and Migration Speeds in Angiogenesis. PLOS Comput Biol. 2009;5: e1000445. doi:10.1371/journal.pcbi.1000445

10. Paulsson J, Micke P. Prognostic relevance of cancer-associated fibroblasts in human cancer. Semin Cancer Biol. 2014;25: 61–68. doi:10.1016/j.semcancer.2014.02.006

11. Ewald AJ, Huebner RJ, Palsdottir H, Lee JK, Perez MJ, Jorgens DM, et al. Mammary collective cell migration involves transient loss of epithelial features and individual cell migration within the epithelium. J Cell Sci. 2012;125: 2638–2654. doi:10.1242/jcs.096875

12. Friedl P, Noble PB, Walton PA, Laird DW, Chauvin PJ, Tabah RJ, et al. Migration of coordinated cell clusters in mesenchymal and epithelial cancer explants in vitro. Cancer Res. 1995;55: 4557–4560.

13. Friedl P. Prespecification and plasticity: shifting mechanisms of cell migration. Curr Opin Cell Biol. 2004;16: 14–23. doi:10.1016/j.ceb.2003.11.001

14. Konen J, Summerbell E, Dwivedi B, Galior K, Hou Y, Rusnak L, et al. Image-guided genomics reveals a vascular mimicry during symbiotic collective cancer invasion. Unpublished. 2016;

15. Smale S. On the differential equations of species in competition. J Math Biol. 1976;3: 5–7. doi:10.1007/BF00307854

16. Dhooge A, Govaerts W, Kuznetsov YA, Meijer HGE, Sautois B. New features of the software MatCont for bifurcation analysis of dynamical systems. Math Comput Model Dyn Syst. 2008;14: 147–175. doi:10.1080/13873950701742754

17. Seydel RU. Practical Bifurcation and Stability Analysis. Springer Science & Business Media; 2009.

18. Sulzmaier FJ, Jean C, Schlaepfer DD. FAK in cancer: mechanistic findings and clinical applications. Nat Rev Cancer. 2014;14: 598–610. doi:10.1038/nrc3792

19. The Cancer Genome Atlas Network. Integrated genomic analyses of ovarian carcinoma. Nature. 2011;474: 609–615. doi:10.1038/nature10166

20. The Cancer Genome Atlas Network. Comprehensive molecular portraits of human breast tumours. Nature. 2012;490: 61–70. doi:10.1038/nature11412

21. Sood AK, Armaiz-Pena GN, Halder J, Nick AM, Stone RL, Hu W, et al. Adrenergic modulation of focal adhesion kinase protects human ovarian cancer cells from anoikis. J Clin Invest. 2010;120: 1515–1523. doi:10.1172/JCI40802

22. Ward KK, Tancioni I, Lawson C, Miller NLG, Jean C, Chen XL, et al. Inhibition of focal adhesion kinase (FAK) activity prevents anchorage-independent ovarian carcinoma cell growth and tumor progression. Clin Exp Metastasis. 2013;30: 579–594. doi:10.1007/s10585-012-9562-5

23. Tanjoni I, Walsh C, Uryu S, Tomar A, Nam J-O, Mielgo A, et al. PND-1186 FAK inhibitor selectively promotes tumor cell apoptosis in three-dimensional environments. Cancer Biol Ther. 2010;9: 764–777.

24. Infante JR, Camidge DR, Mileshkin LR, Chen EX, Hicks RJ, Rischin D, et al. Safety, pharmacokinetic, and pharmacodynamic phase I dose-escalation trial of PF-00562271, an inhibitor of focal adhesion kinase, in advanced solid tumors. J Clin Oncol Off J Am Soc Clin Oncol. 2012;30: 1527–1533. doi:10.1200/JCO.2011.38.9346

25. Roberts WG, Ung E, Whalen P, Cooper B, Hulford C, Autry C, et al. Antitumor activity and pharmacology of a selective focal adhesion kinase inhibitor, PF-562,271. Cancer Res. 2008;68: 1935–1944. doi:10.1158/0008-5472.CAN-07-5155

26. Kang Y, Hu W, Ivan C, Dalton HJ, Miyake T, Pecot CV, et al. Role of focal adhesion kinase in regulating YB-1-mediated paclitaxel resistance in ovarian cancer. J Natl Cancer Inst. 2013;105: 1485–1495. doi:10.1093/jnci/djt210

27. Gilbert-Ross M, Konen J, Koo J, Shupe J, Robinson BS, Wiles WG, et al. Targeting adhesion signaling in KRAS, LKB1 mutant lung adenocarcinoma. JCI Insight. 2017;2. doi:10.1172/jci.insight.90487

28. Lu C, Bonome T, Li Y, Kamat AA, Han LY, Schmandt R, et al. Gene alterations identified by expression profiling in tumor-associated endothelial cells from invasive ovarian carcinoma. Cancer Res. 2007;67: 1757–1768. doi:10.1158/0008-5472.CAN-06-3700

29. Jean C, Chen XL, Nam J-O, Tancioni I, Uryu S, Lawson C, et al. Inhibition of endothelial FAK activity prevents tumor metastasis by enhancing barrier function. J Cell Biol. 2014;204: 247–263. doi:10.1083/jcb.201307067

30. Sitohy B, Nagy JA, Dvorak HF. Anti-VEGF/VEGFR Therapy for Cancer: Reassessing the Target. Cancer Res. 2012;72: 1909–1914. doi:10.1158/0008-5472.CAN-11-3406

31. Folkman J. Tumor angiogenesis: therapeutic implications. N Engl J Med. 1971;285: 1182–1186. doi:10.1056/NEJM197111182852108

32. Inai T, Mancuso M, Hashizume H, Baffert F, Haskell A, Baluk P, et al. Inhibition of vascular endothelial growth factor (VEGF) signaling in cancer causes loss of endothelial fenestrations, regression of tumor vessels, and appearance of basement membrane ghosts. Am J Pathol. 2004;165: 35–52. doi:10.1016/S0002-9440(10)63273-7

33. Kim ES, Serur A, Huang J, Manley CA, McCrudden KW, Frischer JS, et al. Potent VEGF blockade causes regression of coopted vessels in a model of neuroblastoma. Proc Natl Acad Sci U S A. 2002;99: 11399–11404. doi:10.1073/pnas.172398399

34. Hayes DF. Bevacizumab Treatment for Solid Tumors: Boon or Bust? JAMA. 2011;305: 506–508. doi:10.1001/jama.2011.57

35. Hurwitz H, Fehrenbacher L, Novotny W, Cartwright T, Hainsworth J, Heim W, et al. Bevacizumab plus Irinotecan, Fluorouracil, and Leucovorin for Metastatic Colorectal Cancer. N Engl J Med. 2004;350: 2335–2342. doi:10.1056/NEJMoa032691

36. Basanta D, Anderson ARA. Exploiting ecological principles to better understand cancer progression and treatment. Interface Focus. 2013;3. doi:10.1098/rsfs.2013.0020

37. Hardin G. The Competitive Exclusion Principle. Science. 1960;131: 1292–1297. doi:10.1126/science.131.3409.1292

38. Huston M. A General Hypothesis of Species Diversity. Am Nat. 1979;113: 81–101. doi:10.1086/283366

39. D H Boucher, S James, Keeler and KH. The Ecology of Mutualism. Annu Rev Ecol Syst. 1982;13: 315–347. doi:10.1146/annurev.es.13.110182.001531

40. Stachowicz JJ. Mutualism, Facilitation, and the Structure of Ecological CommunitiesPositive interactions play a critical, but underappreciated, role in ecological communities by reducing physical or biotic stresses in existing habitats

and by creating new habitats on which many species depend. BioScience. 2001;51: 235–246. doi:10.1641/0006-3568(2001)051[0235:MFATSO]2.0.CO;2

41. Bauer AL, Jackson TL, Jiang Y. A cell-based model exhibiting branching and anastomosis during tumor-induced angiogenesis. Biophys J. 2007;92: 3105–3121. doi:10.1529/biophysj.106.101501

42. Schaller G, Meyer-Hermann M. Multicellular tumor spheroid in an off-lattice Voronoi-Delaunay cell model. Phys Rev E. 2005;71: 051910. doi:10.1103/PhysRevE.71.051910

43. Shirinifard A, Gens JS, Zaitlen BL, Popławski NJ, Swat M, Glazier JA. 3D Multi-Cell Simulation of Tumor Growth and Angiogenesis. PLOS ONE. 2009;4: e7190. doi:10.1371/journal.pone.0007190

44. Haney S, Reya T, Bazhenov M. Delayed onset of symptoms through feedback interference in chronic cancers. Converg Sci Phys Oncol. 2016;2: 045002. doi:10.1088/2057-1739/2/4/045002

45. Rodriguez-Brenes IA, Komarova NL, Wodarz D. Evolutionary dynamics of feedback escape and the development of stem-cell–driven cancers. Proc Natl Acad Sci. 2011;108: 18983–18988.

46. Lowengrub JS, Frieboes HB, Jin F, Chuang Y-L, Li X, Macklin P, et al. Nonlinear modelling of cancer: bridging the gap between cells and tumours. Nonlinearity. 2010;23: R1. doi:10.1088/0951-7715/23/1/R01

47. Anderson ARA, Weaver AM, Cummings PT, Quaranta V. Tumor morphology and phenotypic evolution driven by selective pressure from the microenvironment. Cell. 2006;127: 905–915. doi:10.1016/j.cell.2006.09.042

48. Liu X, Johnson S, Liu S, Kanojia D, Yue W, Singh UP, et al. Nonlinear Growth Kinetics of Breast Cancer Stem Cells: Implications for Cancer Stem Cell Targeted Therapy. Sci Rep. 2013;3. Available: http://www.nature.com/srep/2013/130820/srep02473/full/srep02473.html?WT.ec_id=SREP-631-20130902

49. Wodarz D, Komarova NL. Dynamics of cancer: mathematical foundations of oncology [Internet]. World Scientific; 2014. Available: https://books.google.com/books?hl=en&lr=&id=90i7CgAAQBAJ&oi=fnd&pg=PR7&dq=Dynamics+of+cancer+komarova&ots=OjSC2djQSP&sig=80eRRrskJ6xbQu0Cnk46GomlyDQ

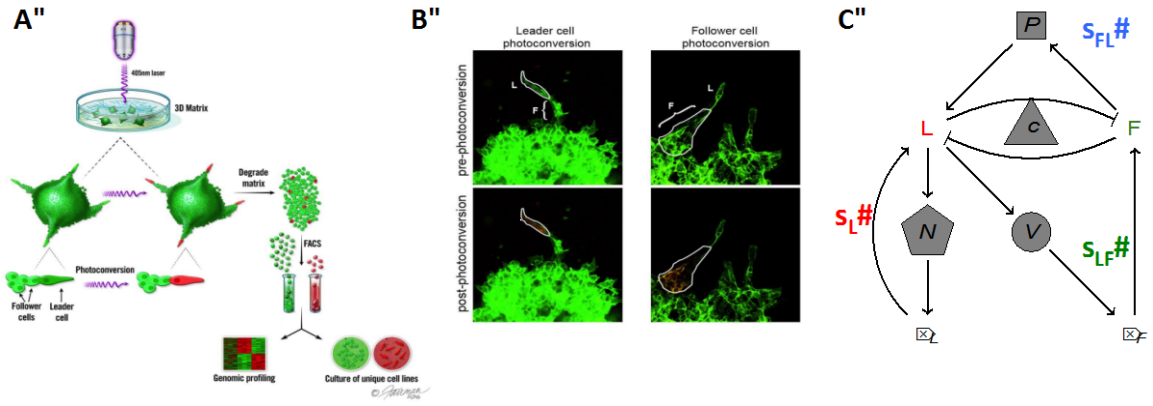

611

612 **Figure 1: Leader and Follower system.** A) Pictorial representation of the spatio-temporal
613 genomic and cellular analysis (SaGA). Adapted from Figure 1 in [14]. B) Photo-conversion
614 examples using 3-D spheroids of H1299-Dendra2 cells. L= leader cell, F = follower cell. Adapted
615 from Figure 1 in [14]. C) Stick representation of mathematical model of leader and follower cell
616 interactions and invasion.

617

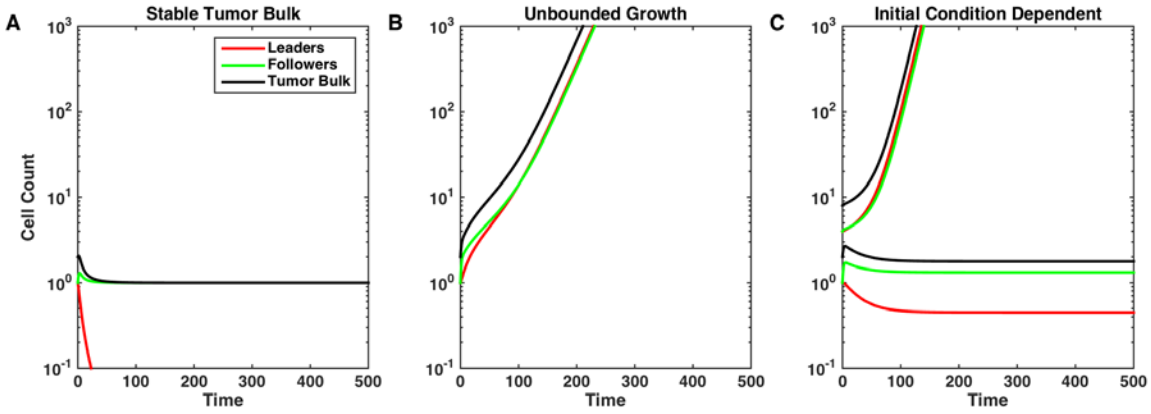

Figure 2: Tumor dynamics depend strongly on feedback strength. Tumor bulk is defined as the sum of leader and follower populations. Tumors may attain a stable size (A: $s_L = 1.2$, $c = 0.6$), grow unboundedly (B: $s_L = 1.2$, $c = 0.05$), or be dependent on initial conditions (C: $s_L = 2$, $c = 0.375$).

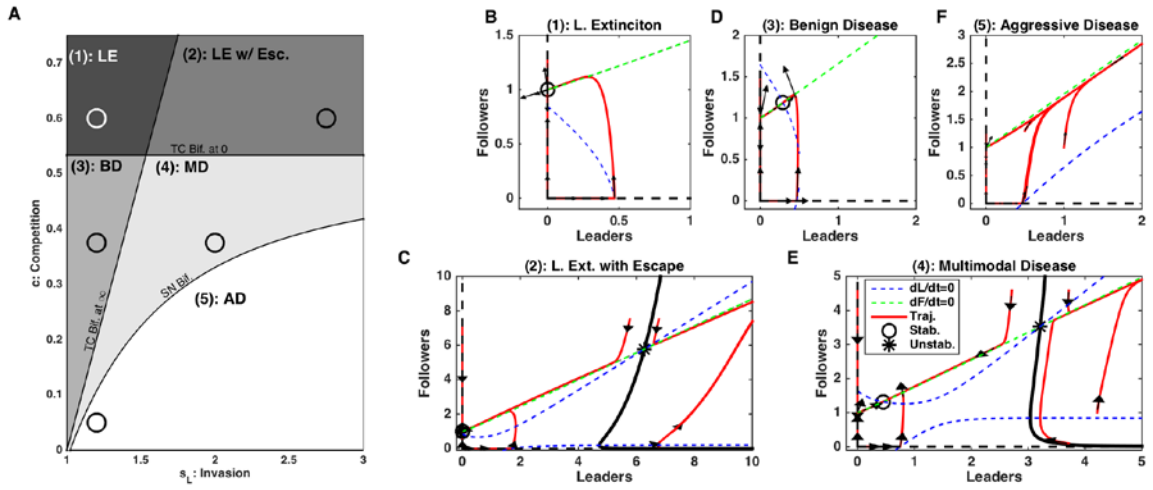

Figure 3: Dynamics of leader and follower ecosystem. A) Bifurcation diagram sweeping feedback strengths s_L and c. Abbreviations - LE: Leader Extinction, LE w/ Esc.: Leader Extinction with Escape, BD: Benign Disease, MD: Multimodal Disease, AD: Aggressive Disease, TC Bif. at ∞: Transcritical Bifurcation at infinity (see Model), TC Bif. at 0: Transcritical Bifurcation at zero (see Model), SN Bif.: Saddle Node Bifurcation (see Model). B-E) Phase diagrams for each of the regimes in A). Dashed blue and green lines are null-clines for the leaders and followers, respectively. Red curves show the trajectories of the leader follower system from different initial conditions, with arrows denoting tangent vectors at various points. Open circles denote stable equilibrium points, stars denote unstable equilibria. Specific s_L and c parameters used are given by the circles in A).

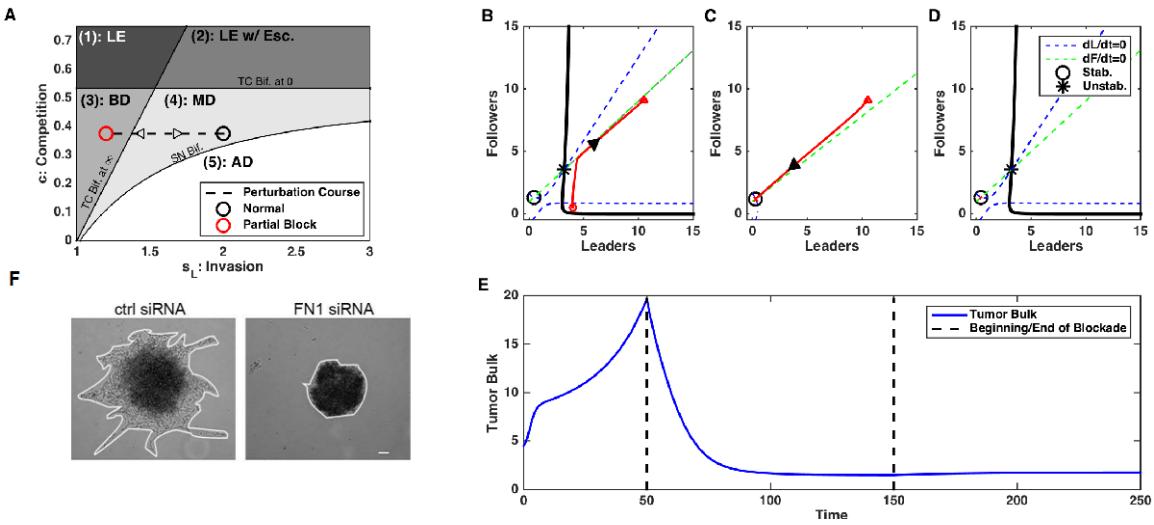

636

637 **Figure 4: Blocking s_L in Multi-modal disease can have irreversible consequences**. A)
638 Bifurcation diagram depicting the direction of the perturbation in parameter space. B-D) Phase plot
639 of tumor dynamics before (B), during (C), and after (D) blockade of s_L. E) Time-course of tumor
640 bulk before, during, and after perturbation. F) Impact on invasion of leader cell cultures during
641 siRNA block of focal adhesion kinase. Reproduced from [14].

642

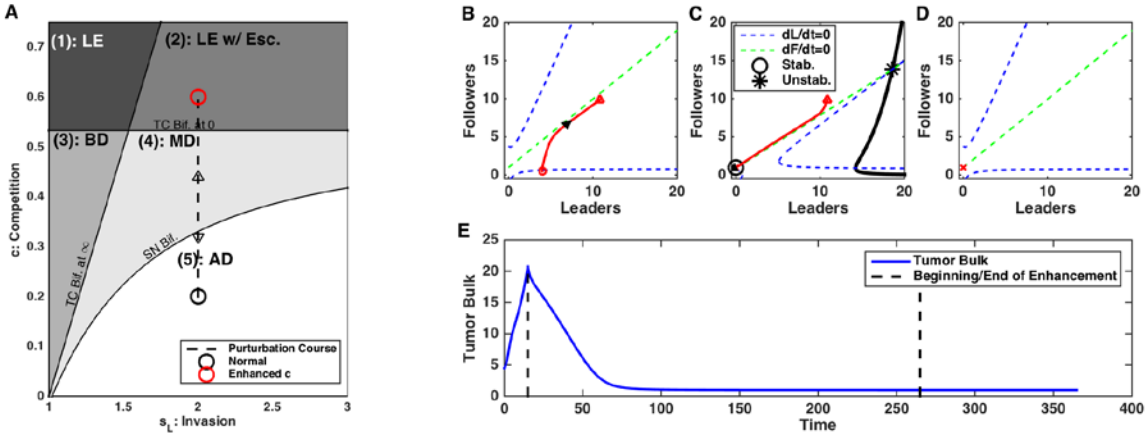

643

644 **Figure 5: Enhancing competition can drive permanent extinction of leaders.** A) Bifurcation
645 diagram depicting the direction of the perturbation in parameter space. B-D) Phase plot of tumor
646 dynamics before (B), during (C), and after (D) enhancement of *c*. E) Time-course of tumor bulk.
647 Here, we assume total extinction of leaders occurs during treatment, i.e. at some point during
648 treatment $L=0$.

649

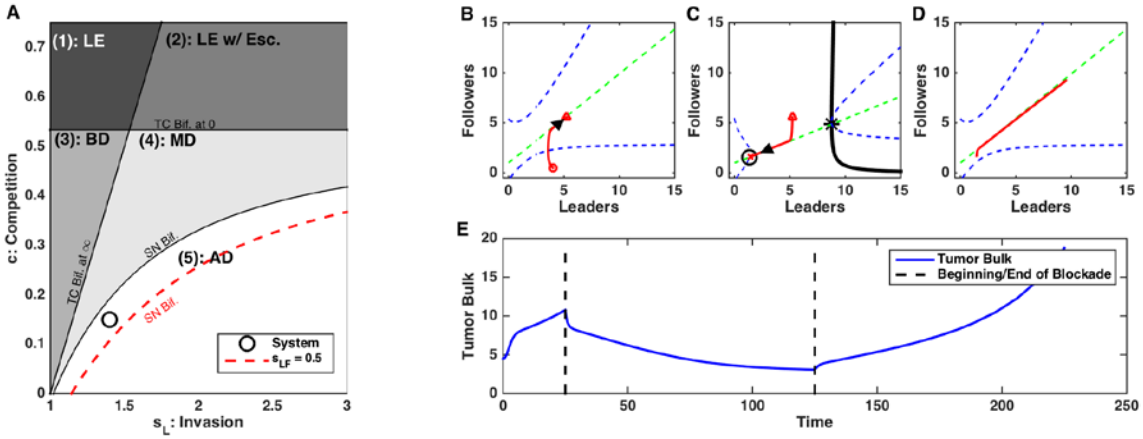

Figure 6: Disrupting Leader to Follower feedback, s_{LF}, can have transient changes in tumor dynamics. A) Bifurcation diagram depicting the direction of the perturbation in parameter space. Perturbations in s_{LF} change the location of the saddle node bifurcation. B-D) Phase plot of tumor dynamics before (B), during (C), and after (D) blockade of s_{LF}. E) Time-course of tumor bulk.

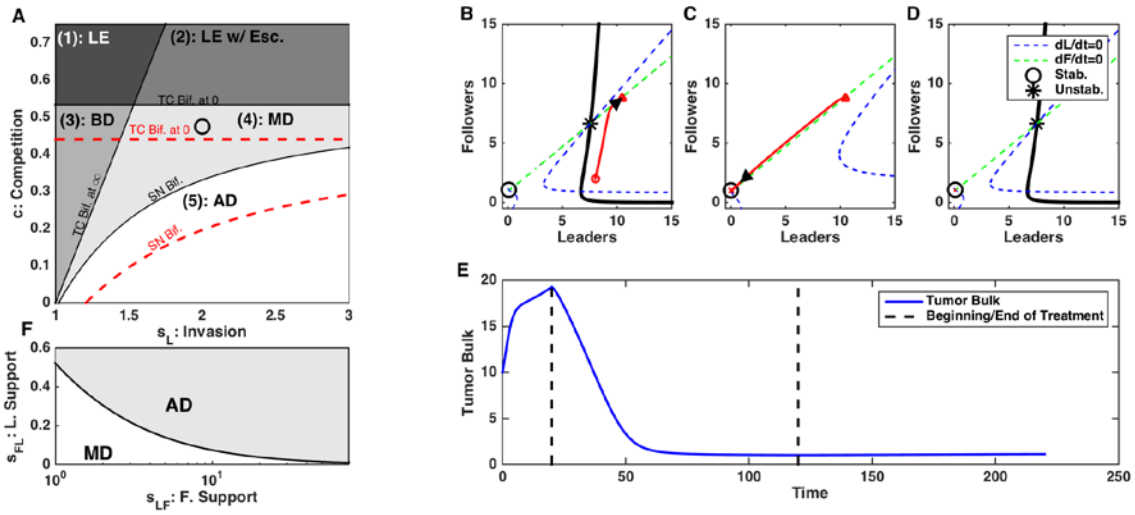

657

658 **Figure 7: Disrupting Follower to Leader feedback, s_{FL}, can have irreversible changes in**
659 **tumor dynamics leading to stabilization of tumor bulk.** A) Bifurcation diagram depicting the
660 direction of the perturbation in parameter space. Perturbations in s_{FL} change the location of the
661 saddle node bifurcation and transcritical bifurcation at zero. B-D) Phase plot of tumor dynamics
662 before (B), during (C), and after (D) blockade of s_{FL}. E) Time-course of tumor bulk. F) Bifurcation
663 diagram depicting the impact of the saddle node bifurcation as a function of s_{LF} and s_{FL}. AD:
664 Aggressive Disease; MD: Multi-modal Disease.

665

666

667